Proc. Natl. Acad. Sci. USA
Vol. 89, pp. 11416–11420, December 1992
Biochemistry

RAD25 (SSL2), the yeast homolog of the human xeroderma pigmentosum group B DNA repair gene, is essential for viability

(excision repair/DNA helicase/preferential repair/Cockayne syndrome)

EUN PARK*, SAMI N. GUZDER†, MARCEL H. M. KOKEN‡, IRIS JASPERS-DEKKER‡, GEERT WEEDA‡, JAN H. J. HOEIJMAKERS‡, SATYA PRAKASH†, AND LOUISE PRAKASH*

*Department of Biophysics, University of Rochester School of Medicine, Rochester, NY 14642; †Department of Biology, University of Rochester, Rochester, NY 14627; and ‡Department of Cell Biology and Genetics, Medical Genetics Center, Erasmus University, P.O. Box 1738, 3000 DR Rotterdam, The Netherlands

Communicated by Allan M. Campbell, September 4, 1992

ABSTRACT **Xeroderma pigmentosum (XP) patients are extremely sensitive to ultraviolet (UV) light and suffer from a high incidence of skin cancers, due to a defect in nucleotide excision repair. The disease is genetically heterogeneous, and seven complementation groups, A–G, have been identified. Homologs of human excision repair genes *ERCC1*, *XPDC/ERCC2*, and *XPAC* have been identified in the yeast *Saccharomyces cerevisiae*. Since no homolog of human *XPBC/ERCC3* existed among the known yeast genes, we cloned the yeast homolog by using *XPBC* cDNA as a hybridization probe. The yeast homolog, *RAD25 (SSL2)*, encodes a protein of 843 amino acids (M_r 95,356). The *RAD25 (SSL2)*- and *XPBC*-encoded proteins share 55% identical and 72% conserved amino acid residues, and the two proteins resemble one another in containing the conserved DNA helicase sequence motifs. A nonsense mutation at codon 799 that deletes the 45 C-terminal amino acid residues in RAD25 (SSL2) confers UV sensitivity. This mutation shows epistasis with genes in the excision repair group, whereas a synergistic increase in UV sensitivity occurs when it is combined with mutations in genes in other DNA repair pathways, indicating that *RAD25 (SSL2)* functions in excision repair but not in other repair pathways. We also show that *RAD25 (SSL2)* is an essential gene. A mutation of the Lys^{392} residue to arginine in the conserved Walker type A nucleotide-binding motif is lethal, suggesting an essential role of the putative RAD25 (SSL2) ATPase/DNA helicase activity in viability.**

In human, xeroderma pigmentosum (XP) is an autosomal recessive disorder, and cells from XP individuals are defective in the incision step of excision repair. Cell fusion studies have indicated the existence of 7 excision-deficient XP complementation groups, A–G (1–3); in addition, at least 10 complementation groups have been identified among UV-sensitive excision-defective rodent cell lines (4–6). Five human genes—*ERCC1*, *ERCC2*, *ERCC3*, *ERCC5*, and *ERCC6*—have been cloned by cross-complementation of UV sensitivity of rodent cell lines (7–11). In addition, the human *XPAC* gene was isolated by complementation of the excision defect of XP-A cell lines (12). *ERCC1* does not complement any of the XP cell lines (13), whereas *ERCC2* and *ERCC3* restore normal excision repair to XP-D and XP-B mutant cell lines (9, 14), respectively, indicating some degree of overlap between the XP and *ERCC* genes.

At least 10 genes are involved in excision repair in the yeast *Saccharomyces cerevisiae*. Mutations in 6 of these genes—*RAD1*, *RAD2*, *RAD3*, *RAD4*, *RAD10*, and *RAD14*—cause extreme UV sensitivity and a defect in the incision step of excision repair (15, 16). The other four genes—*RAD7*, *RAD16*, *RAD23*, and *MMS19*—affect the proficiency of excision repair (15). Many of the yeast excision repair genes are multifunctional, and they play diverse roles in other cellular processes. For example, *RAD3* is essential for viability (17, 18) and *RAD1* and *RAD10* function in mitotic recombination (19, 20). The RAD3 and RAD10 proteins have been purified and characterized in our laboratory. RAD3 is a single-stranded DNA-dependent ATPase, and it possesses DNA and DNA·RNA helicase activities (21–23). Mutational inactivation of RAD3 ATPase/helicase activities renders cells UV-sensitive and defective in excision repair but has no effect on viability (24). The RAD10 protein binds preferentially to single-stranded DNA and it promotes the renaturation of complementary strands of DNA (25).

The yeast *RAD3*, *RAD10*, and *RAD14* genes are homologs of human *XPDC/ERCC2*, *ERCC1*, and *XPAC* genes, respectively (6–9, 16). Since none of the known yeast genes showed homology to the human *XPBC/ERCC3* gene (designated *XPBC* in this paper), we cloned the yeast homolog by using *XPBC* cDNA as a hybridization probe. The yeast homolog has been cloned independently as a suppressor of blocked translation initiation due to the presence of a stem–loop structure in the 5′ untranslated region of *HIS4* mRNA, and those workers have named the gene *SSL2* (26). A mutation in the C-terminal region of the protein encoded by the yeast gene renders cells UV-sensitive, and this mutation shows epistasis with genes of the excision repair group. Because of the requirement of the yeast homolog in DNA repair, and following the convention of nomenclature for yeast DNA repair genes, we have named this gene *RAD25*. Our studies with a genomic deletion mutation indicate that *RAD25* is an essential gene. The *RAD25*-encoded protein shows homology to DNA helicases, and a change of the residue Lys^{392} to arginine in the Walker type A nucleotide-binding sequence motif results in lethality, suggesting that the putative RAD25 ATPase/DNA helicase activity is indispensable for viability.§

MATERIALS AND METHODS

Cloning and Nucleotide Sequence Determination of the *S. cerevisiae RAD25* Gene. Southern blot hybridization of *S. cerevisiae* genomic DNA under low-stringency salt conditions with a 5′ and a 3′ *XPBC* cDNA probe spanning the first two-thirds and last third of the *XPBC* open reading frame, respectively, indicated extensive sequence homology of *XPBC* cDNA with yeast DNA. Several clones of the yeast *XPBC* homolog were identified by low-stringency hybridization of a genomic *S. cerevisiae* λ EMBL3 library with these probes (27).

The publication costs of this article were defrayed in part by page charge payment. This article must therefore be hereby marked "*advertisement*" in accordance with 18 U.S.C. §1734 solely to indicate this fact.

Abbreviations: XP, xeroderma pigmentosum; CS, Cockayne syndrome.

§The sequence reported in this paper has been deposited in the GenBank data base (accession no. L01414).

For nucleotide sequence determination, DNA fragments were cloned into M13 derivative phages and the sequence of both strands of *RAD25* was determined by the dideoxy chain-termination method (28, 29).

Yeast Strains and Media. The *S. cerevisiae* strains used in this study are given in Table 1. Media and conditions for determining UV survival were as previously described (27).

Plasmids and Generation of Yeast *rad25* Mutant Strains. The *RAD25* gene was inserted as a *Hin*dIII–*Bam*HI fragment into the *CEN URA3* low-copy plasmid YCp50 and into a YCp50 derivative in which the *TRP1* gene replaced the *URA3* gene, generating plasmids pEP23 and pEP39, respectively. pEP22 contains the $rad25_{799am}$ mutant allele cloned into the *URA3* integrating vector YIp5 from which the *Sph* I site had been removed. The $rad25_{799am}$ mutation was generated by insertion of a T residue between codons 797 and 798 by site-directed oligonucleotide mutagenesis of the 1.46-kilobase (kb) *Sph* I–*Bam*HI DNA fragment encoding the terminal 249 amino acids of the 843-residue RAD25 protein. Codons 797–799 in the wild type *RAD25* gene are GCC-GTT-AGA, whereas in the $rad25_{799am}$ mutant gene, the corresponding codons are GCC-**T**GT-TAG-A, where **T** is the inserted residue. The $rad25_{799am}$ mutation changes codon 798 from GTT (Val) to TGT (Cys), which is followed by the amber nonsense codon, TAG. Thus, in addition to a change at amino acid 798, the mutant protein differs from the wild-type protein in lacking the 45 C-terminal amino acid residues. The $rad25_{799am}$ mutation was used to replace the wild-type *RAD25* allele in strain DBY747 by transformation to Ura^+ with linearized plasmid pEP22 followed by screening for Ura^- by 5-fluoro-orotic acid (5-FOA) resistance and for UV sensitivity, yielding the haploid strain, EPY88. Genomic deletion mutations of the *RAD1*, *RAD6*, and *RAD52* genes in the $rad25_{799am}$ strain EPY88 were made as described (16), confirmed by allelism tests with known *rad* mutations, and designated EPY90, EPY91, and EPY92, respectively (Table 1).

To generate a genomic deletion mutation of *RAD25*, we used pEP24, a pUC19-based plasmid which contains the flanking *RAD25* sequences and in which the 2.2-kb *Nco* I–*Stu* I DNA fragment located entirely within the *RAD25* open reading frame has been replaced by the yeast *LEU2* gene on a 2.1-kb DNA fragment. Transformation of Leu^- yeast strains to Leu^+ with a *Hin*dIII–*Bgl* II fragment, which contained 726 nucleotides of 5′ flanking sequence and 59 N-terminal codons of *RAD25*, the yeast *LEU2* gene followed by 46 C-terminal *RAD25* codons, and 590 nucleotides of 3′ flanking sequence of *RAD25*, produced a genomic *rad25*Δ mutation. This *rad25*Δ mutation lacked 738 of the 843 codons present in *RAD25*. The *rad25 Arg*^{392} mutation, which results in a change of Lys^{392} to Arg in the Gly-Lys-Thr nucleotide-binding motif, was obtained by site-directed oligonucleotide mutagenesis of the 1.94-kb *Bal* I–*Sph* I fragment of the *RAD25* gene and replacement of the corresponding wild-type *RAD25* DNA segment by the fragment carrying the Arg^{392} mutation, generating the *rad25 Arg*^{392} *CEN URA3* plasmid pPM147.

RESULTS

Nucleotide Sequence of *RAD25*. Nucleotide sequence analysis indicated that *RAD25* encoded a protein of 843 amino acids of M_r 95,356 (Fig. 1). While this paper was in preparation, the nucleotide sequence of the yeast homolog of *XPBC* was published (26). Our data agree with the reported sequence, except for differences at amino acid positions 9 and 48, where our results indicate a serine and a leucine, respectively, instead of proline and serine. In addition, we have noted several nucleotide differences between the two sequences.

Homology Between Yeast *RAD25* and Human *XPBC*-Encoded Proteins. The protein encoded by the yeast *RAD25* gene contains an N-terminal extension of 50 amino acids not present in the XPBC protein; otherwise, the two proteins share extensive homology, with 55% identical residues, and 72% similar residues when identical and conserved changes are grouped together (Fig. 1). RAD25 resembles XPBC in containing the seven conserved sequence motifs that are found in proteins that bind and hydrolyze nucleotides and possess DNA or RNA helicase activities (30). The homology between the two proteins is particularly striking in these domains (Fig. 1). Domain I contains the conserved Walker type A sequence Gly-Xaa-Gly-Lys-Thr/Ser [GXGK(T/S)] (31). At residues 389–393, RAD25 contains the sequence GAGKT, and at residues 343–347 in XPBC, the corresponding sequence is GAGKS. The conserved lysine (K) in the GK(T/S) sequence is involved in interactions with the α phosphoryl group of the bound nucleotide (32). Domain II contains the Walker type B sequence motif, where three to five conservative hydrophobic amino acids are followed by an aspartate residue (31). This sequence occurs at residues 479–493 in RAD25, and at residues 432–446 in XPBC. Aspartate in this sequence has been proposed to interact with Mg^{2+} on MgATP, and the hydrophobic residues serve to exclude water from the ATP reaction center (32). The role of other conserved sequence motifs in helicases is not known.

RAD25 Contains Sequence Motifs Characteristic of DNA Helicases but Not of RNA Helicases. Both DNA and RNA helicases have the same sequences in motif I but they differ in the sequences in motifs II and VI. Fig. 2 shows a comparison of helicase sequence motifs I, II, and VI among RAD25, RAD3, and eIF-4A. The *S. cerevisiae* RAD3 protein is a single-stranded DNA-dependent ATPase, and it possesses DNA and DNA·RNA helicase activities (21–23). RAD3 does not hydrolyze ATP in the presence of RNA cofactors and it has no RNA helicase activity (23). eIF-4A is a eukaryotic translation initiation factor and it possesses an RNA helicase activity that is capable of unwinding mRNAs (33). eIF-4A belongs to a family of proteins, many of which have been shown to possess RNA-dependent ATPase and

Table 1. *S. cerevisiae* strains

Strain	Genotype
EPY59	*MAT***a** *ade2-1 arg4-8 cyhl0*^{R} *his4-280 leu2-27 trp1*Δ *ura3-1*
EPY60	*MATα ade2-1 his4-260 leu2-3,112 trp1*Δ *ura3-1*
EPY61	EPY59 × EPY60 (*RAD25/RAD25*)
EPY62	EPY61 carrying a *rad25*Δ mutation in one of the homologs (*RAD25/rad25*Δ::*LEU2*)
DBY747	*MAT***a** *his3-*Δ*1 leu2-3,112 trp1-289 ura3-52*
EPY88	DBY747 with $rad25_{799am}$ mutation replacing the genomic *RAD25* gene
EPY90	EPY88*rad1*Δ::*URA3*
EPY91	EPY88*rad6*Δ::*URA3*
EPY92	EPY88*rad52*Δ::*URA3*

The gene symbol following the double colon (::) indicates the yeast selectable marker used in generating the *rad*Δ mutation.

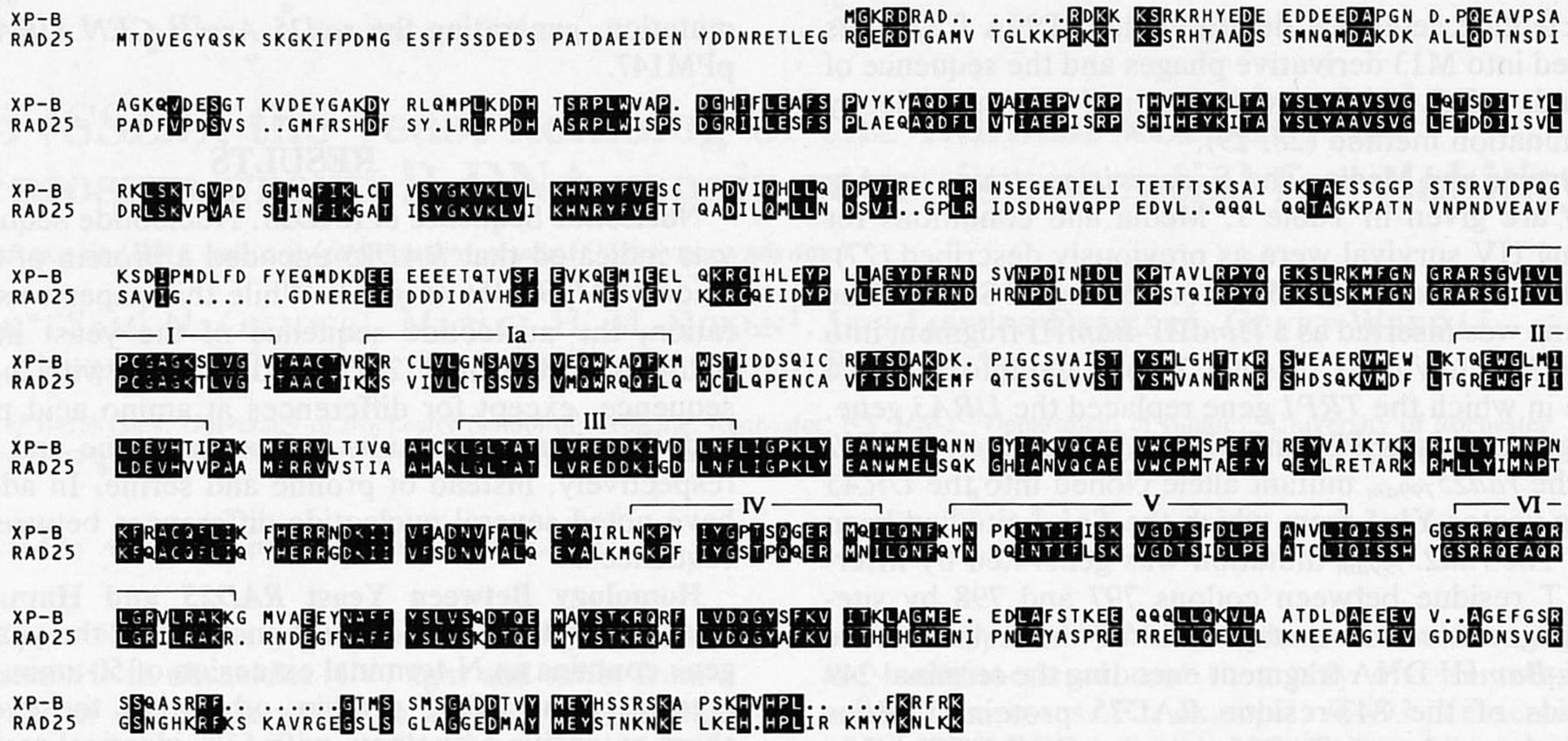

FIG. 1. Homology between the human XPBC (9) and *S. cerevisiae* RAD25 proteins. The two amino acid sequences were aligned by using the BESTFIT program of the Genetics Computer Group, Madison, WI. Identical residues are indicated by white lettering on black background. The helicase consensus sequences (30) are denoted by horizontal lines with Roman numerals (I, Ia, II–VI) above the sequences.

RNA helicase activities, and they all share the sequence motif DEAD in domain II and HRIGR in domain VI (34, 35). These two motifs are absent from known DNA helicases, including RAD3. RAD25 also lacks the DEAD and HRIGR sequence motifs, suggesting that RAD25 possesses the DNA-dependent ATPase and DNA helicase activities but neither the ability to hydrolyze ATP or other nucleotides in the presence of RNA nor an RNA helicase activity.

***RAD25* Is an Essential Gene.** Mutations in the human *XPBC* gene or in the equivalent gene in rodent cell lines cause a defect in excision repair of UV-damaged DNA. However, since genomic deletion mutations of several yeast DNA repair genes have uncovered additional functions not identified in previous studies with the missense mutations, we made a genomic deletion mutation of *RAD25* and examined its effect on cell viability. The RAD^+/RAD^+ diploid strain EPY61 was transformed with a linear DNA fragment that contained the 5′ and 3′ flanking sequences of *RAD25* and only a small portion of the open reading frame and in which the internal 2.2-kb segment of the *RAD25* open reading frame was replaced by the yeast *LEU2* gene. The generation of a deletion mutation in the *RAD25* gene in one of the homologs and its replacement by *LEU2* were confirmed by Southern blot analysis (data not shown). Genetic analysis of tetrads following sporulation of the *RAD25*/*rad25*Δ::*LEU2* diploid strain EPY62 revealed no asci with three or four viable spores. Of 91 tetrads examined, 70 produced two viable spores and 21 produced one viable spore. In addition, all spores recovered from EPY62 were UV-resistant and none were Leu^+, indicating that *rad25*Δ::*LEU2* spores are inviable. In contrast, the RAD^+/RAD^+ strain EPY61 produced tetrads containing three or four viable spores. Thus, *RAD25* is an essential gene.

Assignment of *RAD25* to the Excision Repair Epistasis Group. The human *XP11BE* mutation, which causes a defect in excision repair, is due to the insertion of 4 base pairs (bp) at the splice junction of the last intron/exon, and it produces a frameshift resulting in a protein with an alteration of the 43 C-terminal residues (9). To examine the role of *RAD25* in DNA repair in yeast, we constructed a mutation, $rad25_{799am}$, by inserting a T residue between codons 797 and 798. This frameshift mutation changes amino acid residue 798 from valine to cysteine, and because of the amber nonsense codon at position 799, the encoded protein is predicted to lack the 45 C-terminal amino acids. As expected, the $rad25_{799am}$ mutation conferred UV sensitivity on yeast, indicating an involvement of *RAD25* in DNA repair. In *S. cerevisiae*, the UV DNA repair genes belong to any of the three epistasis groups. The *RAD3* group consists of excision repair genes; genes in the *RAD6* epistasis group function in postreplication repair of UV-damaged DNA and in damage-induced mutagenesis, and genes in the *RAD52* group are involved in double-strand break repair and recombination. Since *RAD25* is essential for cell viability, its role in DNA repair could be more general than just an involvement in excision repair. To examine the possibility that *RAD25* functions in more than one pathway of DNA repair, we constructed double mutant combinations of $rad25_{799am}$ with a *rad*Δ mutation from each of the epistasis groups and compared the UV sensitivity of single and double mutants. In combination with the excision-defective *rad1*Δ mutation, we observed an epistatic relationship, since the UV survival of the $rad25_{799am}$ *rad1*Δ double mutant was the same as that of the *rad1*Δ mutant (Fig. 3*A*). In contrast, a synergistic decline in UV survival occurred when the $rad25_{799am}$ mutation was combined with either the *rad6*Δ (Fig. 3*B*) or the *rad52*Δ (Fig. 3*C*) mutation. These results indicate an involvement of *RAD25* in excision repair and not in other repair processes. The lower level of UV sensitivity of the $rad25_{799am}$ mutation than that of the totally excision defective *rad1*Δ mutation could reflect the fact that *RAD25* is not absolutely required for excision repair. Alternatively, the $rad25_{799am}$ mutation might be leaky because of

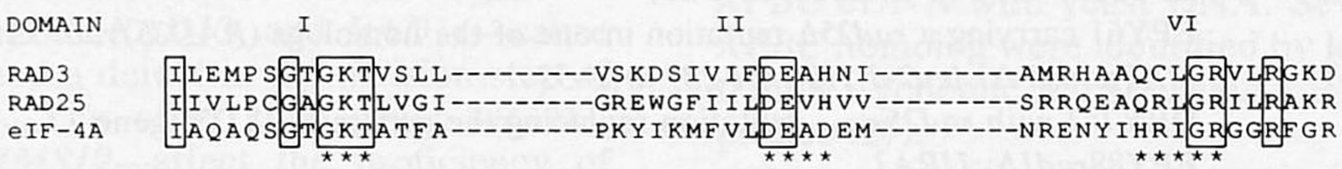

FIG. 2. Comparison of RAD25 with RAD3, a DNA helicase, and the eukaryotic translation initiation factor eIF-4A, an RNA helicase, in domains I, II, and VI of the seven conserved domains found in the superfamilies of helicases. Identical residues shared among all three proteins are boxed. The GKT box present in all three proteins, and the DEAD box and the HRIGR sequence motifs present in eIF-4A but not in RAD3 or RAD25 are denoted by stars.

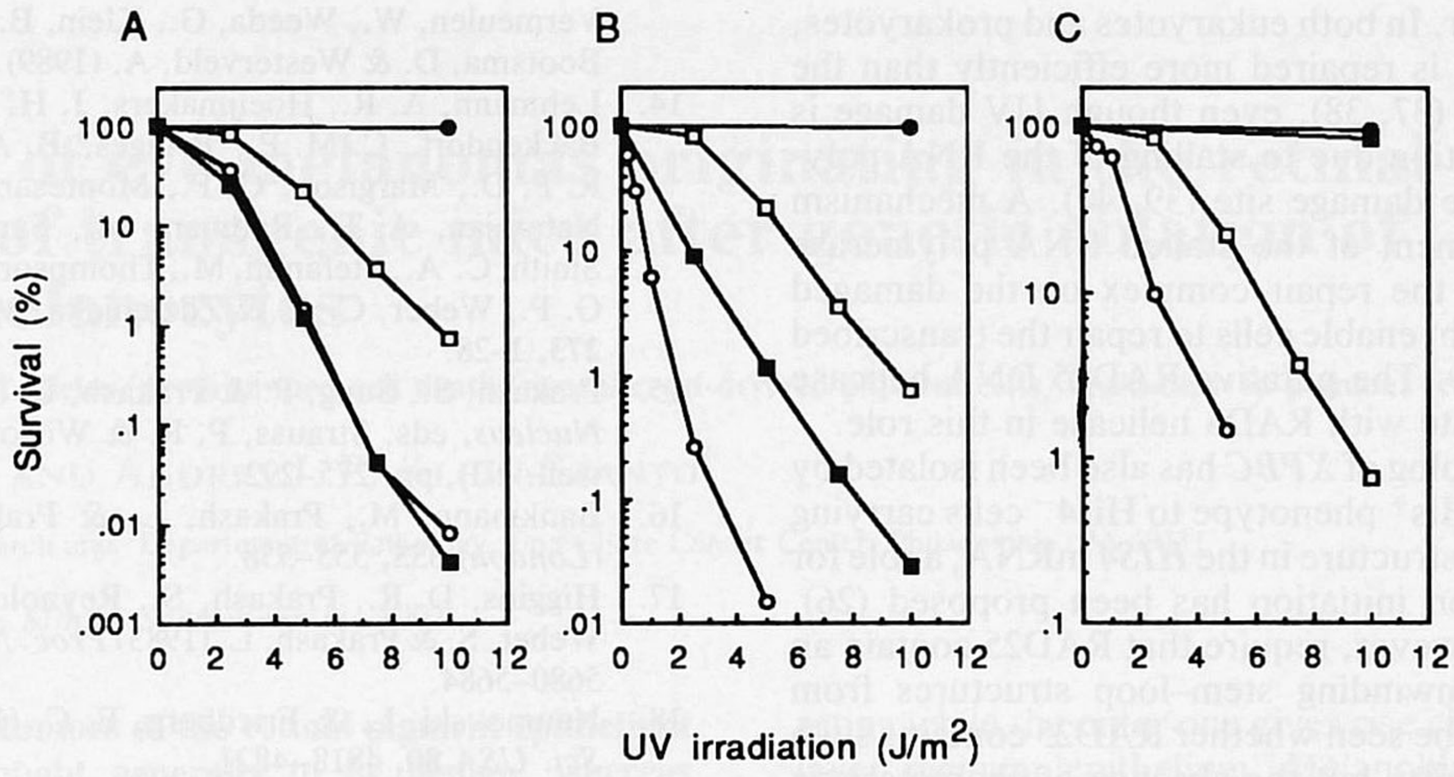

FIG. 3. Survival after UV irradiation of *RAD*$^+$ strain DBY747 and its isogenic derivatives bearing deletions of various *RAD* genes. (*A*) ●, *RAD*$^+$; □, *rad25*$_{799am}$; ■, *rad1*Δ; ○, *rad25*$_{799am}$*rad1*Δ. (*B*) ●, *RAD*$^+$; □, *rad25*$_{799am}$; ■, *rad6*Δ; ○, *rad25*$_{799am}$ *rad6*Δ. (*C*) ●, *RAD*$^+$; □, *rad25*$_{799am}$; ■, *rad52*Δ; ○, *rad25*$_{799am}$*rad52*Δ. Survival curves represent an average of three experiments for each strain.

low-level frameshifting resulting in small amounts of normal protein.

Lethality of the *rad25 Arg*^{392} Mutation. Mutation of Lys^{48} to arginine in the GKT Walker type A sequence motif in RAD3 results in loss of ATPase, DNA helicase, and DNA·RNA helicase activities but not of the ability to bind ATP or single-stranded DNA (23, 24). This mutation does not affect the cell viability function of RAD3 but renders cells UV-sensitive and defective in excision repair (24). To examine the biological role of the putative ATPase/DNA helicase activity in RAD25, we mutated Lys^{392} in the GKT sequence to arginine. Since we were unable to obtain a genomic replacement of the wild-type *RAD25* allele with the *rad25 Arg*^{392} mutant allele, we considered the possibility that this mutation might be lethal. To test this, the *RAD25*/*rad25*Δ::*LEU2* diploid strain EPY62 was transformed with either the *RAD25* gene or the *rad25 Arg*^{392} mutation carried on the *CEN URA3* plasmids pEP23 and pPM147, respectively. As expected, genetic analysis following sporulation of EPY62 transformed with pEP23 (*RAD25*) revealed many tetrads with four and three viable spores, and 35% (41/116) of the spores were Leu$^+$, and they all carried the *RAD25* plasmid pEP23, indicating the restoration of viability to the *rad25*Δ::*LEU2* spores by the *RAD25* plasmid. In contrast, in the 60 tetrads analyzed from EPY62 carrying the *rad25 Arg*^{392} plasmid pPM147, none contained more than two viable spores, and none of the spores were Leu$^+$, indicating that the *rad25 Arg*^{392} mutant gene does not complement the inviability defect of the *rad25*Δ::*LEU2* spores. Sixty-three percent (60/96) of the *RAD25* spores contained the *rad25 Arg*^{392} plasmid pPM147, and these spores grew normally, indicating that the *rad25 Arg*^{392} mutant gene has no effect on viability of wild-type *RAD25* cells. The *rad25 Arg*^{392} mutation, therefore, is recessive lethal. In summary, our results suggest a vital role for the putative ATPase/DNA helicase activity in RAD25.

DISCUSSION

The yeast *RAD25* gene shows a high degree of homology to the human *XPBC* gene, and both genes resemble one another in their role in DNA repair. A frameshift mutation in *XPBC* that alters the 43 C-terminal amino acids renders cells UV-sensitive and defective in the incision step of excision repair (9). The epistatic relationship of the *rad25*$_{799am}$ mutation encoding a protein lacking the 45 C-terminal amino acids with genes in the excision repair group and not with genes that function in other repair pathways is consistent with the involvement of *RAD25* in excision repair. It is highly probable that like *XPBC*, *RAD25* is also required for incision. Thus, the products of at least seven genes—*RAD1*, *RAD2*, *RAD3*, *RAD4*, *RAD10*, *RAD14*, and *RAD25*—may be indispensable for incision of UV-damaged DNA in yeast.

In addition to its requirement in excision repair, *RAD25* is essential for cell viability. In this respect, *RAD25* resembles *RAD3*, which is also required for excision repair and cell viability. The DNA repair and viability functions in *RAD3* are mutationally separable, suggesting that different segments of RAD3 interact with different protein components in carrying out these two functions. Since the *rad25*$_{799am}$ mutation affects the DNA repair but not the viability function, in RAD25 also, the domains affecting these functions might reside in different portions of the protein. The C terminus of RAD25, and of XPBC, could be specifically involved in interactions with the protein components of the incision complex.

Both XPBC and RAD25 contain the conserved domains found in proteins that bind and hydrolyze nucleotides. A comparison of these domains in RAD25 with those present in RAD3, which possesses DNA and DNA·RNA helicase activities, and with eIF-4A, an RNA helicase, suggests that RAD25 (and also XPBC) possesses a DNA helicase activity. In this aspect too, RAD25 appears to resemble RAD3. However, our studies indicate that the RAD3 and the putative RAD25 DNA helicase activities differ in regard to their roles in DNA repair and viability. A mutation of Lys^{48} to arginine in the Walker type A consensus sequence of RAD3 results in a protein devoid of any ATPase, DNA helicase, or DNA·RNA helicase activity (23, 24). The *rad3 Arg*^{48} mutation has no effect on viability but confers an extreme sensitivity to UV light and a defect in excision repair (24). In contrast, as shown in this study, a similar conservative change of the Lys^{392} residue to arginine in the Walker type A nucleotide-binding motif in RAD25 is lethal, implicating an indispensable role of RAD25 ATPase/DNA helicase activities in viability.

In addition to suffering from the characteristic symptoms of XP, XP-B and many XP-D patients exhibit clinical features of another DNA repair disorder, Cockayne syndrome (CS) (3, 9). Since both XP and CS disorders are extremely rare, their simultaneous occurrence in these patients is very likely the result of the mutation in the *XPBC* or the *XPDC* gene. CS can also occur without the accompaniment of XP. CS patients suffer from severe dwarfism and mental retardation, and they show premature aging. CS cells are sensitive to UV light and are defective in the preferential repair of actively transcribed genes (36). The association of XP-B and XP-D with CS suggests a role for XPBC and XPDC proteins and their yeast homologs in providing a link between transcrip-

tion and excision repair. In both eukaryotes and prokaryotes, the transcribed strand is repaired more efficiently than the nontranscribed strand (37, 38), even though UV damage is inhibitory to transcription due to stalling of the RNA polymerase complex at the damage site (39, 40). A mechanism that couples displacement of the stalled RNA polymerase with the assembly of the repair complex on the damaged transcribed strand might enable cells to repair the transcribed strand more efficiently. The putative RAD25 DNA helicase activity may collaborate with RAD3 helicase in this role.

Since the yeast homolog of *XPBC* has also been isolated by its ability to restore a His^+ phenotype to $His4^-$ cells carrying an artificial stem–loop structure in the *HIS4* mRNA, a role for this gene in translation initiation has been proposed (26). Such a role would, however, require that RAD25 contain an activity capable of unwinding stem–loop structures from mRNAs. It remains to be seen whether RAD25 contains such an RNA helicase activity, but the absence of characteristic RNA helicase sequence motifs in RAD25 argues against such a possibility.

We thank E. Miller and M. Sweet for excellent technical assistance, P. Sung for reading the manuscript, and R. Johnson for sequence alignment. This work was supported by Grants DE-FGO2-88ER60621 from the Department of Energy and CA41261 and CA35035 from the National Institutes of Health and by the Dutch Cancer Society (Project IKR 88-02 and 90-20), the European Community (Contract B16-141-NL), and the Council for Medical Research of the Netherlands Organization for Scientific Research (Contract 900-501-091).

1. Cleaver, J. E. & Kraemer, K. H. (1989) in *The Metabolic Basis of Inherited Disease*, eds. Scriver, C. R., Beaudet, A. L., Sly, W. S. & Valle, D. (McGraw–Hill, New York), Vol. 2, pp. 2949–2971.
2. De Weerd-Kastelein, E. A., Keijzer, W. & Bootsma, D. (1972) *Nature (London) (New Biol.)* **238,** 80–83.
3. Vermeulen, W., Stefanini, M., Giliani, S., Hoeijmakers, J. H. J. & Bootsma, D. (1991) *Mutat. Res.* **255,** 201–208.
4. Thompson, L. H., Shiomi, T., Salazar, E. P. & Stewart, S. A. (1988) *Somatic Cell Mol. Genet.* **14,** 605–612.
5. Stefanini, M., Collins, A. R., Riboni, R., Klaude, M., Botta, E., Mitchell, D. L. & Nuzzo, F. (1991) *Cancer Res.* **51,** 3965–3971.
6. Hata, H., Numata, M., Tohda, H., Yasui, A. & Oikawa, A. (1991) *Cancer Res.* **51,** 195–198.
7. Van Duin, M., de Wit, J., Odijk, H., Westerveld, A., Yasui, A., Koken, M. H. M., Hoeijmakers, J. H. J. & Bootsma, D. (1986) *Cell* **44,** 913–923.
8. Weber, C. A., Salazar, E. P., Stewart, S. A. & Thompson, L. H. (1990) *EMBO J.* **9,** 1437–1447.
9. Weeda, G., Van Hamm, R. C. A., Vermeulen, W., Bootsma, D., van der Eb, A. J. & Hoeijmakers, J. H. J. (1990) *Cell* **62,** 777–791.
10. Mudgett, J. S. & MacInnes, M. A. (1990) *Genomics* **8,** 623–633.
11. Troelstra, C., Odijk, H., de Wit, J., Westerveld, A., Thompson, L. H., Bootsma, D. & Hoeijmakers, J. H. J. (1990) *Mol. Cell. Biol.* **10,** 5806–5813.
12. Tanaka, K., Miura, N., Satokata, I., Miyamoto, I., Yoshida, M. C., Satoh, Y., Kondo, S., Yasui, A., Okayama, H. & Okada, Y. (1990) *Nature (London)* **348,** 73–76.
13. Van Duin, M., Vredeveldt, G., Mayne, L. V., Odijk, H., Vermeulen, W., Weeda, G., Klein, B., Hoeijmakers, J. H. J., Bootsma, D. & Westerveld, A. (1989) *Mutat. Res.* **217,** 83–92.
14. Lehmann, A. R., Hoeijmakers, J. H. J., van Zeeland, A. A., Backendorf, C. M. P., Bridges, B. A., Collins, A., Fuchs, R. P. D., Margison, G. P., Montesano, R., Moustacchi, E., Natarajan, A. T., Radman, M., Sarasin, A., Seeberg, E., Smith, C. A., Stefanini, M., Thompson, L. H., van der Schans, G. P., Weber, C. A. & Zdzienicka, M. Z. (1992) *Mutat. Res.* **273,** 1–28.
15. Prakash, S., Sung, P. & Prakash, L. (1990) in *The Eukaryotic Nucleus*, eds. Strauss, P. R. & Wilson, S. H. (Telford, Caldwell, NJ), pp. 275–292.
16. Bankmann, M., Prakash, L. & Prakash, S. (1992) *Nature (London)* **355,** 555–558.
17. Higgins, D. R., Prakash, S., Reynolds, P., Polakowska, R., Weber, S. & Prakash, L. (1983) *Proc. Natl. Acad. Sci. USA* **80,** 5680–5684.
18. Naumovski, L. & Friedberg, E. C. (1983) *Proc. Natl. Acad. Sci. USA* **80,** 4818–4821.
19. Schiestl, R. H. & Prakash, S. (1988) *Mol. Cell. Biol.* **8,** 3619–3626.
20. Schiestl, R. H. & Prakash, S. (1990) *Mol. Cell. Biol.* **10,** 2485–2491.
21. Sung, P., Prakash, L., Weber, S. & Prakash, S. (1987) *Proc. Natl. Acad. Sci. USA* **84,** 6045–6049.
22. Sung, P., Prakash, L., Matson, S. W. & Prakash, S. (1987) *Proc. Natl. Acad. Sci. USA* **84,** 8951–8955.
23. Bailly, V., Sung, P., Prakash, L. & Prakash, S. (1991) *Proc. Natl. Acad. Sci. USA* **88,** 9712–9716.
24. Sung, P., Higgins, D., Prakash, L. & Prakash, S. (1988) *EMBO J.* **7,** 3263–3269.
25. Sung, P., Prakash, L. & Prakash, S. (1992) *Nature (London)* **355,** 743–745.
26. Gulyas, K. D. & Donahue, T. F. (1992) *Cell* **69,** 1031–1042.
27. Reynolds, P., Koken, M. H. M., Hoeijmakers, J. H. J., Prakash, S. & Prakash, L. (1990) *EMBO J.* **9,** 1423–1430.
28. Sanger, F., Nicklen, S. & Coulson, A. R. (1977) *Proc. Natl. Acad. Sci. USA* **74,** 5463–5467.
29. Biggin, M. D., Gibson, T. J. & Hong, G. F. (1983) *J. Biol. Chem.* **134,** 315–319.
30. Gorbalenya, A. E., Koonin, E. V., Donchenko, A. P. & Blinov, V. L. (1989) *Nucleic Acids Res.* **17,** 4713–4730.
31. Walker, J. E., Saraste, M., Runswick, M. J. & Gay, N. J. (1982) *EMBO J.* **1,** 945–951.
32. Fry, D. C., Kuby, S. A. & Mildvan, A. S. (1986) *Proc. Natl. Acad. Sci. USA* **83,** 907–911.
33. Ray, B. K., Laeson, T. G., Kramer, J. C., Cladaras, M. H., Grifo, J. A., Abramson, R. D., Merrick, W. C. & Thach, R. T. (1985) *J. Biol. Chem.* **260,** 7651–7658.
34. Linder, P., Lasko, P. F., Ashburner, M., Leroy, P., Nielson, P. J., Nishi, K., Schnier, J. & Slonimski, P. O. (1989) *Nature (London)* **337,** 121–122.
35. Kim, S.-H., Smith, J., Claude, A. & Lin, R.-J. (1992) *EMBO J.* **11,** 2319–2326.
36. Venema, J., Mullenders, L. H. F., Natarajan, A. T., Van Zeeland, A. A. & Mayne, L. V. (1990) *Proc. Natl. Acad. Sci. USA* **87,** 4707–4711.
37. Mellon, I., Spivak, G. & Hanawalt, P. C. (1987) *Cell* **51,** 241–249.
38. Mellon, I. & Hanawalt, P. C. (1989) *Nature (London)* **342,** 95–98.
39. Sauerbier, W. & Hercules, K. (1978) *Annu. Rev. Genet.* **12,** 329–363.
40. Selby, C. P. & Sancar, A. (1990) *J. Biol. Chem.* **265,** 21330–21336.

Proc. Natl. Acad. Sci. USA
Vol. 89, pp. 11421–11425, December 1992
Medical Sciences

Malignancy of eye melanomas originating in the retinal pigment epithelium of transgenic mice after genetic ablation of choroidal melanocytes

(*Kit/W, W^v* mutant alleles/programmed cell death/neural crest-derived pigment cells/brain-derived pigment cells)

BEATRICE MINTZ* AND ANDRES J. P. KLEIN-SZANTO†

*Institute for Cancer Research and †Department of Pathology, Fox Chase Cancer Center, Philadelphia, PA 19111

Contributed by Beatrice Mintz, September 11, 1992

ABSTRACT **Eye tumors of the retinal pigment epithelium (RPE) have been thought generally to be benign, whereas choroidal ones are malignant. To test this assumption in mice, the *W/W^v* (*Kit*) mutant genotype was introduced into melanoma-prone transgenic mice whose recombinant simian virus 40 transforming sequences are specifically expressed in pigment cells. *W/W^v* causes programmed death of neural crest-derived pigment cells, including choroidal ones, but leaves intact the brain-derived pigment cells, such as those in the RPE. Dysplastic cells arose in the RPE, contiguous with frank melanotic neoplasms. Invasion of the optic nerve, and tumor growth outside the orbit, attested to the malignancy of these RPE-derived melanomas. The widespread melanosis previously seen in mice with this transgene was absent when *W/W^v* was added, thus validating its chief origin from neural crest cells.**

Ocular melanomas may arise from any of the pigmented tissues of the eye: the choroid, ciliary body, or iris (together comprising the uveal tract), or the retinal pigment epithelium (RPE). In humans, choroidal melanomas are the most common type and are generally malignant (1, 2). Human RPE tumors are said to be difficult to diagnose (3), especially as eye tumors tend to be seen at late stages; most of them are benign and their status as melanomas has been questioned. In the melanoma-susceptible transgenic mice that we have produced, malignant eye melanomas appeared to originate from the RPE as well as from the other possible target tissues (4). [The transgene, designated Tyr-SV40E in those experiments, is activated by the pigment cell-specific tyrosinase promoter, which drives the simian virus 40 (SV40) early-region sequences, including the T-antigen transforming gene.] Nevertheless, in advanced disease in the mice, multiple displaced tumors often coexisted in an eye, and contributions from the initially neighboring RPE and choroidal layers could then no longer be distinguished. It was thus of interest to determine whether mouse eye tumors arising from the RPE could be clearly shown to be malignant and to compare the potential for RPE malignancy in mouse and human.

We decided upon genetic ablation of choroidal melanocytes in the transgenic mice, as this would obviate occurrence of choroidal melanomas. Such a strategy is feasible because choroidal and retinal pigment cells develop from separate sources and are separately affected by specific mutant genes (5). The neural crest normally provides migratory dendritic melanocytes to the skin and hair follicles, to the choroid layer of the eye, and to several other tissues (6). The brain is the other source of pigment cell precursors. The optic vesicles arise as paired bulb-like outpocketings of the forebrain. Each indents to form a double-layered cup whose innermost layer develops into the highly complex neural retina while the outer one gives rise chiefly to the single-cell-layer pigment epithelium. Melanoblasts originating in the neural crest populate the choroid on the opposite flank of the RPE. The RPE then serves in part as a polarized transport system, functionally linking the vascular network of the choroid with the neural retina. Some mutations at the *W* (white-spotting) locus lead to programmed death of neural crest-derived—but not brain-derived—pigment cells, failure of germ-cell proliferation and survival, and macrocytic anemia (7). *W/W^v* is one of the genotypes of mice with black eyes, white coat, and severe anemia (6). The animals are usually inviable unless reconstituted with healthy hematopoietic tissue; they are also presumptively sterile. The locus, now termed *Kit*, has been found to encode a transmembrane growth factor receptor with tyrosine kinase activity; both *W* and *W^v* alleles have been isolated and sequenced (8, 9).

MATERIALS AND METHODS

To incorporate *W/W^v* into our Tyr-SV40E transgenic mice (4), the sterility due to *W/W^v* requires that the *W* and *W^v* alleles be introduced separately in a series of matings. Moreover, the limited viability of *W/W^v* due to severe macrocytic anemia (6) necessitates early rescue by repopulation with normal hematopoietic cells.

All mice in the experiment were congenic with the C57BL/6 inbred strain. Individuals either hemizygous for the T-antigen-encoding transgene (*Tag/−*) or homozygous (*Tag/Tag*) were all from line 9, described in the earlier report (4). The transgene in this line is not linked to the *W* locus (data not shown). In the following series of matings, only the segregants of interest are indicated:

(*i*) *W/+* × *Tag/Tag* → *W/+;Tag/−*, etc.

(*ii*) *W^v/+* × *Tag/Tag* → *W^v/+;Tag/−*, etc.

(*iii*) *W/+;Tag/−* × *W^v/+;Tag/−* → *W/W^v;Tag/Tag*, *W/W^v;Tag/−*, etc. *W/W^v* mice, recognizable by their extreme pallor, were reconstituted at birth by intravenous inoculation with adult bone marrow cells, as described (10). Marrow donors with the β-globin *Hbb^d* genetic variant were used, to distinguish donor-derived erythropoiesis from that of the recipients (*Hbb^s*), in electrophoretic analyses of blood to monitor successful repopulation. Healthy *W/W^v* survivors that were hemi- or homozygous for the transgene were identified by DNA analysis of tail tissue (4).

Tissues prepared for histology were fixed in formalin and embedded in paraffin; the sections were stained with hematoxylin and eosin.

RESULTS

Candidate Mice. The transgene was previously found to reduce the content of both eumelanin (black/brown) and phaeomelanin (yellow) pigments in the coat (4). The

The publication costs of this article were defrayed in part by page charge payment. This article must therefore be hereby marked "*advertisement*" in accordance with 18 U.S.C. §1734 solely to indicate this fact.

Abbreviations: RPE, retinal pigment epithelium; SV40, simian virus 40.

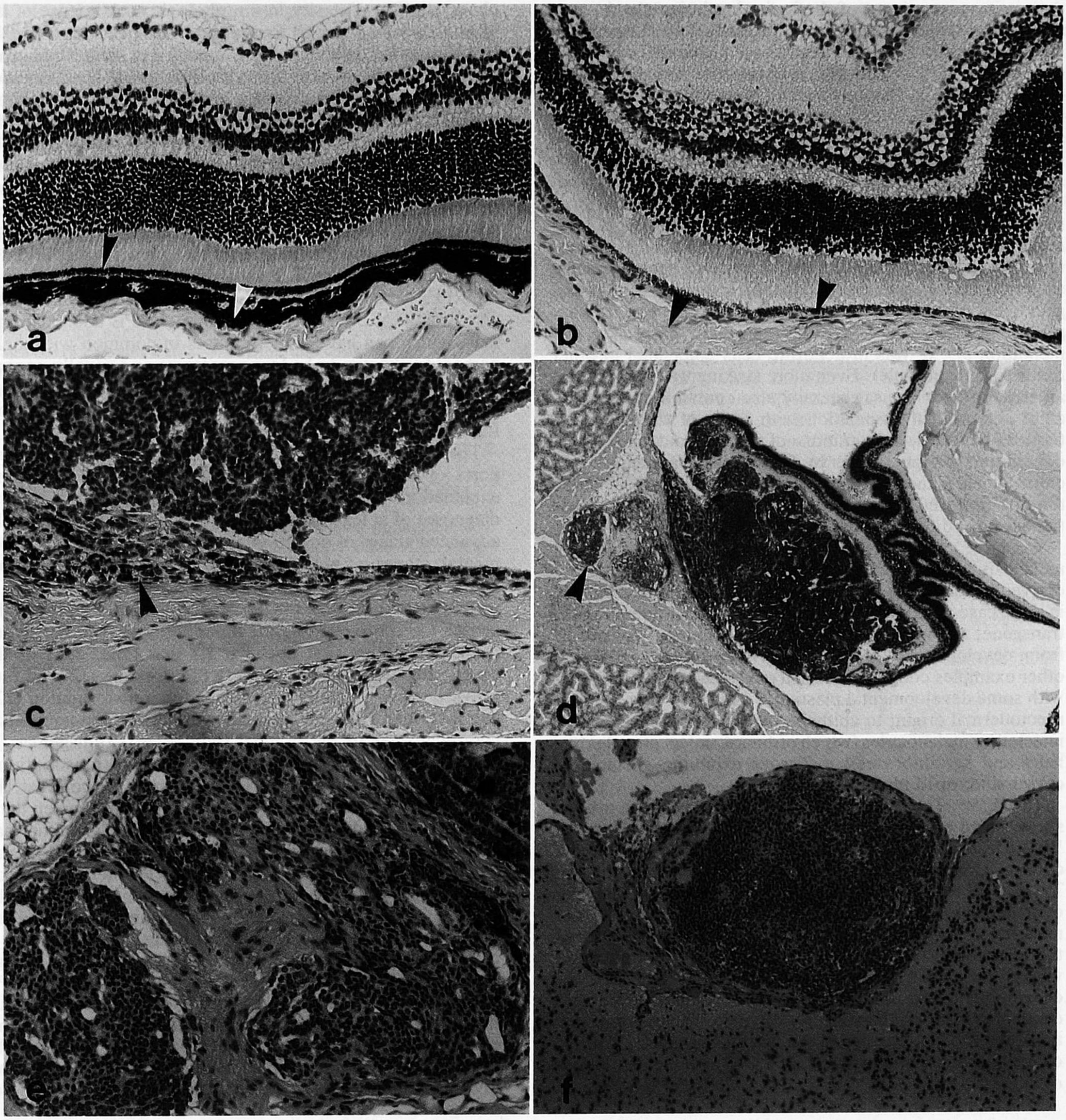

FIG. 4. (*a*) Normal eye section of a 14-week control C57BL/6 mouse showing the neural retina and, below it, the RPE (left arrowhead) and the melanocytic cells of the choroid (right arrowhead), with intense melanin deposition in both. (*b*) Eye of a 24-week W/W^v-C57BL/6 nontransgenic animal. No melanocytic cells are present in the choroid (left arrowhead). The RPE (right arrowhead) is less pigmented than in younger W/W^v or wild-type mice. (*c*) Retina of a 24-week W/W^v mouse hemizygous for the Tyr-SV40E transgene (*Tag*/−). A hyperplastic area (arrowhead) of the hypomelanotic RPE is contiguous with the hypomelanotic early melanoma above. (*d*) In a 17-week W/W^v mouse homozygous for the transgene (*Tag*/*Tag*), a melanoma has arisen in the papillary area of the RPE and has caused retinal detachment. Tumor cells have invaded the optic nerve (arrowhead). (*e*) Higher magnification of the same tumor, showing invasion in the optic nerve. Some melanoma cells are intensely pigmented. (*f*) Tumor nodule in the base of the skull of the same animal. (Hematoxylin/eosin stain; *a*–*c*, and *e*, ×100; *d*, ×20; *f*, ×40.)

of all three transgenic mice with W/W^v. The melanomas were hypopigmented and arose in focally hypopigmented and dysplastic regions of the RPE. The contiguity of an early melanoma and a hyperplastic RPE region is evident in Fig. 4*c*. The melanomas were poorly differentiated and were chiefly epithelioid, with some spindle and glanduliform areas, and with sporadically distributed pigmentation.

Malignancy of RPE Melanomas. At more advanced stages, the RPE melanomas had invaded the optic nerve. In the case shown (Fig. 4 *d* and *e*), the main tumor mass caused extensive retinal detachment and displacement. Tumor had also invaded, or metastasized to, the base of the skull (Fig. 4*f*).

Lack of Melanosis in Tyr-SV40E Mice with W/W^v. The occurrence of melanized cells in tissues ordinarily lacking melanin, or producing relatively small amounts, is referred to as melanosis or melanocytosis. Apart from the usual presence of melanin-containing cells in the skin and eyes, moderate numbers of pigmented cells are often found in mice in

the nictitans, meninges of the brain, harderian glands, parathyroids, thymus (5), inner ear (15), and spleen. Only in one mouse strain, PET (now extinct), have pigmented cells been seen more widely distributed, in connective tissues throughout the body (16). The existence of melanosis in Tyr-SV40E transgenic mice (17) therefore came as a surprise, especially as the transgene caused a reduction rather than an increase in coat pigmentation, and the ocular and cutaneous melanomas in the same animals tended to be hypo- rather than hyperpigmented (4). In those individuals, melanosis was seen, with decreasing frequency, in the following novel sites: nasal mucosa, endocardium, lungs, peripheral nervous system, lymph nodes, central nervous system, genital organs, skeletal muscle, oral mucosa, tooth enamel organ, pineal gland, choroid plexus, mammary glands, larynx, salivary glands, bladder, and urethra (17). In many cases, the pigmentation *per se* was in dendritic cells embedded in other tissue (e.g., in muscle). Even more striking was the fact that an array of neoplasms, generally also containing some melanin, occurred in association with some of the melanotic tissues. Included were tumors of the choroid plexus, endocardium, peripheral nerve sheath (schwannomas), cochlea, pineal gland, salivary gland, and nasal mucosa. These tumors appeared to be distinct from peripheral melanotic tumors judged to be metastases of eye melanomas (4, 17).

We have proposed (17) that most of the examples of melanosis and associated tumors represent neural crest-derived melanocytes that had increased in number, and had in some cases become transformed, under the influence of the transgene; the melanocytic schwannomas may have come from developmentally bipotential neural crest cells. The other examples could be ascribed to epithelia and endothelia with some developmental plasticity, especially those of neuroectodermal origin; to epithelia receiving melanin granules injected by melanocytes (which ordinarily inject granules into hairs and keratinocytes); to tissues exhibiting metaplastic conversion; or to phagocytic cells.

The $W/W^v;Tag/-$ (or $W/W^vTag/Tag$) mice in the present study afford an opportunity to test those interpretations, as W/W^v leads to programmed cell death (18, 19) of melanocytes originating in the neural crest, while expression of the Tyr-SV40E transgene causes transformation of cells capable of melanization. The animals examined to date do in fact lack melanosis as well as the tumors previously associated with that condition. Thus the new evidence lends support to the view of melanosis as primarily an aberration of neural crest development. The lack of cutaneous melanomas reflects the death of skin melanoblasts in W/W^v mice. The transgene has apparently failed to override the deleterious effect of W/W^v on melanoblast viability, possibly due to a greater expression of W/W^v.

DISCUSSION

The results unambiguously demonstrate that melanotic neoplasms can originate from the RPE *in vivo* and can become malignant. Dysplastic cells, representing premalignant changes of the RPE, were seen contiguous with full-fledged malignant melanomas, under genetic conditions precluding origin from the choroid. Invasion of the optic nerve and presence of tumor outside the orbit attest to the malignant nature of the RPE-derived tumors. Their designation as melanomas is supported by their origin from melanized cells and is more specific than a broader designation based on their epithelial origin, especially as the RPE is not a conventional lining or glandular epithelium.

The RPE melanomas seen here and previously (4) in the transgenic mice were predominantly hypomelanotic and epithelioid. Nevertheless several other patterns characterized by glanduliform, fusiform, or small-cell differentiation were observed. The diversity in morphologic architecture of human melanomas is well known and has been reviewed by Nakhleh *et al.* (20), who have concluded that "malignant melanomas may assume the histologic guise of adenocarcinomas, small cell carcinomas, and sarcomas." Most of the tumors reviewed by those investigators reacted strongly with the reagents for S-100 protein and the HMB-45 antigen. The fact that these same histological and histochemical characteristics were found in both skin and RPE tumors in our transgenic mice, before the W/W^v genotype was introduced (4), strongly supports the view that the RPE neoplasms are melanomas. Further evidence for this view is their invasive and metastatic potential. It should be noted that no tumor of the RPE, except melanoma, is characterized by this aggressive biological behavior. For example, RPE adenocarcinomas, which can have some features in common with melanomas, are known to be less aggressive and usually nonmetastasizing (21). In addition, the adenocarcinomas produce cytokeratins whereas melanomas, including the eye tumors found in our transgenic mice, are negative for keratin.

The disparity between our observations on mice and reports of human RPE tumors may have several possible explanations: species differences; incorrect or ambiguous diagnoses of at least some human eye tumors (3), due to the advanced stages of detection; or differences in the developmental stages at which the mouse and human tumors arise—at relatively younger and older ages, respectively. In the experimental mice, the tyrosinase promoter undoubtedly causes the transgene to start functioning in fetal life, when eye pigmentation first appears. At that time, cells of the developing eye are most actively proliferating (12) and thus provide many potential target cells for transformation (22); the fact that RPE melanomas were more common than choroidal ones in the original (non-W/W^v) transgenics (4) may be further attributable to differences in transcriptional strength of this promoter in RPE vs. choroid. In contrast, the typically later-onset human eye tumors originate when there is little RPE cell division (23), yet choroidal melanocytes may still be frequently dividing. The difference between human and mouse in occurrence of malignant RPE melanomas may therefore be more apparent than fundamental, with the balance of melanoma formation simply shifting among the different pigmented eye tissues with age, and the RPE in older individuals becoming more likely to form only benign tumors. Nevertheless, any agent capable of stimulating RPE cell division *in vivo* or *in vitro* would be expected to reactivate the potential for malignant RPE melanomas at any age. This expectation is borne out by the fact that explanted RPE cells of adult human and other mammalian species resume active division in culture and can be transformed with virions or oncogenes (24, 25).

Two aspects of RPE aging contribute to an understanding of eye melanoma formation in Tyr-SV40E transgenic mice: pigmentary and mitotic changes. The higher prenatal than postnatal expression of tyrosinase in the RPE would mean that the transgene, driven by a tyrosinase promoter, is likely to initiate RPE melanomas at an early age; melanomas were indeed already present when the eyes were first examined histologically, at 4 weeks (4). Mitotic activity in the C57BL/6 mouse RPE declines soon after birth and cell numbers are stabilized by 2 weeks of age, with some further increase in area due to cell enlargement (12). In light of the age-related reduction in melanization (Figs. 2 and 4*b*), it follows that a stimulus to cell proliferation—in this case, the transforming SV40 sequences—would in effect distribute the available melanosomes among an increasing number of cells, thereby leading to hyperplastic nodules that are hypomelanotic, and to hypomelanotic tumors. This did in fact occur (Fig. 4*c*; also see figure 2 in ref. 4) and was puzzling when first observed.

W/W^v animals containing the integrated Tyr-SV40E transgene can now be used as a source of material with which several questions can be examined. Ostensibly normal RPE cells, destined to become malignant, can be explanted from very young mice to define genetic changes as the cells progress toward malignancy. Whereas unavoidable contamination of RPE cultures with choroidal melanocytes has until now posed a problem for studies *in vitro* (26), no such ambiguity would persist here. The animals themselves will also enable metastatic propensities specific to RPE melanomas to be identified in the absence of any choroidal or skin melanomas.

We thank Nancy Loughery for excellent technical assistance throughout the study and Monika Bradl for DNA verification of the transgene copy number. This work was supported by U.S. Public Health Service Grants CA42560 to B.M. and CA06927 and RR05539 to the Fox Chase Cancer Center, as well as an appropriation to the Center from the Commonwealth of Pennsylvania.

1. Foos, R., Straatsma, B., Gardner, K., Zakka, K. & Omphroy, C. (1983) in *Intraocular Tumors*, eds. Lommatzsch, P. K. & Blodi, F. C. (Springer, Berlin), pp. 51–57.
2. Newell, F. W. (1992) *Ophthalmology Principles and Concepts* (Mosby Year Book, St. Louis), pp. 284–317.
3. Tso, M. O. M. (1979) in *The Retinal Pigment Epithelium*, eds. Zinn, K. & Marmor, M. (Harvard Univ. Press, Cambridge, MA), pp. 267–276.
4. Bradl, M., Klein-Szanto, A., Porter, S. & Mintz, B. (1991) *Proc. Natl. Acad. Sci. USA* **88,** 164–168.
5. Markert, C. L. & Silvers, W. K. (1956) *Genetics* **41,** 429–450.
6. Silvers, W. K. (1979) *The Coat Colors of Mice* (Springer, New York).
7. Mintz, B. & Russell, E. S. (1957) *J. Exp. Zool.* **134,** 207–238.
8. Nocka, K., Majumder, S., Chabot, B., Ray, P., Cervone, M., Bernstein, A. & Besmer, P. (1989) *Genes Dev.* **3,** 816–826.
9. Nocka, K., Tan, J. C., Chiu, E., Chu, T. Y., Ray, P., Traktman, P. & Besmer, P. (1990) *EMBO J.* **9,** 1805–1813.
10. Capel, B. & Mintz, B. (1989) *Exp. Hematol.* **17,** 872–876.
11. Boulton, M. (1991) *Prog. Retinal Res.* **11,** 125–151.
12. Bodenstein, L. & Sidman, R. L. (1987) *Dev. Biol.* **121,** 192–204.
13. Guillery, R. W. & Price, S. D. (1985) in *Biological, Molecular and Clinical Aspects of Pigmentation*, eds. Bagnara, J. T., Klaus, S. N., Paul, E. & Schartl, M. (Univ. Tokyo Press, Tokyo), pp. 303–312.
14. Miyamoto, M. & Fitzpatrick, T. B. (1957) *Science* **126,** 449–450.
15. Deol, M. S. (1970) *Proc. R. Soc. London Ser. A* **175,** 201–217.
16. Nichols, S. E. & Reams, W. M., Jr. (1960) *J. Embryol. Exp. Morphol.* **8,** 24–32.
17. Klein-Szanto, A., Bradl, M., Porter, S. & Mintz, B. (1991) *Proc. Natl. Acad. Sci. USA* **88,** 169–173.
18. Mintz, B. (1970) *Symp. Int. Soc. Cell Biol.* **9,** 15–42.
19. Mintz, B. (1971) *Symp. Soc. Exp. Biol.* **25,** 345–370.
20. Nakhleh, R. E., Wick, M. R., Rocamora, A., Swanson, P. E. & Dehner, L. P. (1990) *Am. J. Clin. Pathol.* **93,** 731–740.
21. Tso, M. O. M. & Albert, D. M. (1972) *Arch. Ophthalmol.* **88,** 27–38.
22. Mintz, B. & Fleischman, R. A. (1981) *Adv. Cancer Res.* **34,** 211–278.
23. Tso, M. O. M. (1968) *Arch. Ophthalmol.* **80,** 214–216.
24. Albert, D. M., Rabson, A. S. & Dalton, A. J. (1968) *Invest. Ophthalmol.* **7,** 357–365.
25. Dutt, K., Scott, M., Del Monte, M., Agarwal, N., Sternberg, P., Srivastava, S. K. & Srinivasan, A. (1990) *Oncogene* **5,** 195–200.
26. Wang, C.-W., Roque, R. S., Defoe, D. M. & Caldwell, R. B. (1991) *Curr. Eye Res.* **10,** 1081–1086.

Proc. Natl. Acad. Sci. USA
Vol. 89, pp. 11426–11427, December 1992
Biophysics

A proposed function for spermine and spermidine: Protection of replicating DNA against damage by singlet oxygen

(singlet oxygen quenching/polyamines)

AHSAN U. KHAN†, YING-HUA MEI‡, AND THÉRÈSE WILSON‡

†Department of Pathology, Harvard Medical School, Boston, MA 02115; and ‡Department of Cellular and Developmental Biology, Harvard University, Cambridge, MA 02138

Communicated by Michael Kasha, August 31, 1992 (received for review February 19, 1992)

ABSTRACT **Like all aliphatic amines, the polyamines spermine and spermidine are physical quenchers of singlet molecular oxygen ($^1O_2^*$). The rate constants of these processes were determined *in vitro* with photochemically generated $^1O_2^*$ and the hydrocarbon rubrene as substrate, in pyridine. At millimolar concentration, spermine and spermidine should quench $^1O_2^*$ *in vivo* and prevent it from damaging DNA. It is proposed that a biological function of polyamines is the protection of replicating DNA against oxidative damage.**

"... spermidine and spermine are widely distributed in nature, but their function is not known with any certainty" (1). This sentence summarizes the status in 1991 of a problem that has been addressed in thousands of papers since Leeuwenhoek's discovery in 1677 of crystals of spermine phosphate in human semen (2), where spermine reaches the amazingly high concentration of 3.3 mg/g. It is known that polyamines (Table 1) slow down autoxidation processes (3–5) and thus inhibit oxidative damage caused by free radicals. We propose here that the primary function of polyamines is to protect DNA and RNA against singlet oxygen, $^1O_2^*$ ($^1\Delta_g$), a highly reactive and long-lived excited state of molecular oxygen. Tertiary and secondary amines are long known to be physical quenchers of singlet oxygen (6, 7). Chemical reaction is minimal, and the amines are therefore not destroyed in the quenching process. Spermidine and spermine (with one and two secondary amine groups, respectively; Table 1) are shown here to be no exception.

The recent paper of Balasundaram *et al.* (1) presents intriguing and unexplained results consistent with our proposal. These authors describe a mutant of *Saccharomyces cerevisiae* in which endogenous putrescine is present in normal levels, but the mutant is unable to synthesize spermine and spermidine and requires their exogenous addition for growth. However, this requirement holds *only* in aerobic conditions, not in an atmosphere of N_2/5% CO_2.

Amine Quenching of Singlet Oxygen

The effectiveness of spermine and spermidine as *in vitro* quenchers of $^1O_2^*$ was determined by their ability to retard the self-sensitized photooxygenation of rubrene (5,6,11,12-tetraphenylnaphthacene), a bright-red hydrocarbon (R) that reacts rapidly with $^1O_2^*$ ($k_r = 4 \times 10^7\ M^{-1}\cdot s^{-1}$) (7) to form a colorless endoperoxide (RO_2). This reaction competes with quenching of $^1O_2^*$ by amine (A):

$$^1O_2^* + R \xrightarrow{k_r} RO_2$$

$$^1O_2^* + A \xrightarrow{k_q} A + {}^3O_2$$

Aerated pyridine solutions of rubrene (0.22 mM) were irradiated at 540 nm, and the concentration of rubrene was followed photometrically as a function of irradiation time, down to a concentration of rubrene of about one-half its initial concentration; this was repeated in the presence of different concentrations of amines in the millimolar range. Under these conditions, k_o/k_A, the ratio of the pseudo-first-order rate constant of decay of rubrene without amine to that with amine, can be treated in a Stern–Volmer fashion. The slopes of plots of k_o/k_A vs. amine concentration is $k_q\tau$, where τ is the lifetime of $^1O_2^*$ in the absence of amine under the conditions of the experiment. These plots are linear up to ≈2 mM in the case of spermine and spermidine.

This procedure was used to determine $k_q\tau$ not only for spermine and spermidine but also for 1,4-diazabicyclo-[2.2.2]octane (DABCO), triethylamine, and diethylamine, three well-studied amines. The relative values are as follows: DABCO and $(C_2H_5)_3N$, 1; spermine, 0.5; spermidine, 0.4; $(C_2H_5)_2NH$, 0.2. The rate constants for $^1O_2^*$ quenching by spermine and spermidine, calculated on the basis of an average literature value (7) of $k_q = 2.5 \times 10^7\ M^{-1}\cdot s^{-1}$ for DABCO, are listed in Table 2. The order of k_q was expected, since it reflects the known order of k_q values of aliphatic amines (7): tertiary (1) > secondary (0.2) > primary (0.005). Amines quench $^1O_2^*$ by a charge-transfer process (6, 8); therefore, the lower the ionization potential, the better the quencher. Similar results were obtained in toluene solution with rose bengal as the sensitizer and irradiation at 560 nm.

Biological Effects of Polyamines

In addition to the recent work with the yeast mutants, earlier studies with *Escherichia coli* mutants deficient in aliphatic polyamines clearly show the importance of these amines for growth (9, 10). In eukaryotes, an indication of their potentially crucial role is the fact that ornithine decarboxylase, the enzyme that catalyzes the first step of polyamine biosynthesis, is synthesized in a burst at the end of the G_1 phase, just before the S (synthesis) phase, and then is rapidly degraded (10). In mammalian cells, it has the fastest protein turnover rate of all eukaryotic enzymes.

There is no firm data on the cellular localization of polyamines *in vivo*, although the timing of the enzymatic synthesis of the polyamines and the high levels of ornithine decarboxylase certainly suggest a role for polyamines at the time of DNA synthesis. *E. coli* mutant studies indicate that polyamines affect the rate of movement of the DNA replicating fork (11). *In vitro* work shows a close association of polyamines with DNA, neutralizing at least in part its negative charges and stabilizing it (12, 13). Similarly, there is evidence for binding of polyamines to RNA (14) and an indication that polyamines increase the fidelity of translation

The publication costs of this article were defrayed in part by page charge payment. This article must therefore be hereby marked "*advertisement*" in accordance with 18 U.S.C. §1734 solely to indicate this fact.

Abbreviation: DABCO, 1,4-diazabicyclo[2.2.2]octane.

Table 1. Structures of some polyamines

Amine	Structure
Putrescine	NH_2-$(CH_2)_4$-NH_2
Spermidine	NH_2-$(CH_2)_3$-NH-$(CH_2)_4$-NH_2
Spermine	NH_2-$(CH_2)_3$-NH-$(CH_2)_4$-NH-$(CH_2)_3$-NH_2

(10). All this is consistent with the proposal that polyamines protect DNA and RNA against attack by $^1O_2^*$.

Many possible sources of $^1O_2^*$ in living cells have been identified, among them peroxidases (15, 16), dismutation (17) of superoxide ion O_2^-, and electron transfer from O_2^- to metals (18, 19). As a result, singlet oxygen like polyamines is ubiquitous. The preferred site for $^1O_2^*$ attack on nucleic acids is the guanine residue. *In vitro*, the rate constant of the reaction with guanine has been estimated (20) at 5.3×10^6 $M^{-1}\cdot s^{-1}$ and that of $^1O_2^*$ with DNA at 5.1×10^5 $M^{-1}\cdot s^{-1}$. These rate constants are both smaller than that for quenching of $^1O_2^*$ by either spermine or spermidine. Therefore, these amines should afford protection to DNA, provided that they are strategically located near the site of $^1O_2^*$ attack, as is expected. Oxidation of guanine in DNA causes loss of transforming activity and mutagenesis, as well as some single-strand breaks (21–23).

In *E. coli*, the concentration of spermidine is reported to be 4.7 μmol/g of wet weight (24). On the assumption of 10^{12} cells per g of wet weight and a cell volume of 2 μm^3, one calculates a spermidine concentration, averaged over the whole cell, of $\approx$2 mM, well within the necessary range for DNA protection. Single-stranded DNA regions with exposed bases are the most likely targets of $^1O_2^*$ attack; if some of the spermidine were synthesized near the replication forks, the local concentration of amine could be much higher. Although putrescine (with only primary amine groups) is expected to be a weaker quencher, its presence may be sufficient to protect DNA in nonreplicating cells of the yeast mutant (1).

Conclusions

The harmful effects of $^1O_2^*$ are, of course, not limited to nucleic acids. Its reactivity with amino acids as well as with lipids, leading to damage to cell membranes, is also well documented (25). In addition, it should be emphasized that $^1O_2^*$ is evidently not the only possible agent of oxidative damage. O_2^-, H_2O_2, and the extremely reactive free radical ·OH must all be considered (26). As mentioned earlier, several studies have shown that polyamines may also intervene in some of these reactions. For example, they retard free-radical autoxidation processes (3–5) and seem to moderate the toxicity of paraquat, a source of superoxide ion (27).

We believe that a case can be made for a role of polyamines in the protection of DNA against oxidative attack, as documented in a companion paper (28), and that this may be their primary function. One might speculate that, downstream, the presence of polyamines could then allow protein synthesis, once the integrity of DNA and RNA was ensured.

The present ideas could have implications for research in fertility.

Table 2. Rate constants, k_q, for $^1O_2^*$ quenching by amines

Amine	k_q,† $M^{-1}\cdot s^{-1} \times 10^{-7}$
$(C_2H_5)_3N$	2.5
DABCO	2.5
Spermine	1.2
Spermidine	1.0
$(C_2H_5)_2NH$	0.5

†Calculated on the basis of an average literature value (7) of 2.5×10^7 $M^{-1}\cdot s^{-1}$ for DABCO.

We thank Konrad Bloch, J. Woodland Hastings, and David B. Wilson for comments on the manuscript.

1. Balasundaram, D., Tabor, C. W. & Tabor, H. (1989) *Proc. Natl. Acad. Sci. USA* **88,** 5872–5876.
2. Leeuwenhoek, A. (1678) *Philos. Trans. R. Soc.* **12,** 1040.
3. Tabor, H., Tabor, C. W. & Rosenthal, S. M. (1961) *Annu. Rev. Biochem.* **30,** 579–604.
4. Tadolini, B., Cabrini, L., Landi, L., Varini, E. & Pasqualini, P. (1984) *Biochem. Biophys. Res. Commun.* **122,** 550–555.
5. Lovaas, E. (1991) *J. Am. Oil Chem. Soc.* **68,** 353–358.
6. Ouannès, C. & Wilson, T. (1968) *J. Am. Chem. Soc.* **90,** 6527–6528.
7. Monroe, B. M. (1985) in *Singlet O2*, ed. Frimer, A. A. (CRC, Boca Raton, FL), Vol. 1, pp. 177–224.
8. Furukawa, M. S., Gray, E. W. & Ogryzlo, E. A. (1970) *Ann. N.Y. Acad. Sci.* **171,** 175–185.
9. Cohen, S. S. (1971) *Introduction to the Polyamines* (Prentice-Hall, Englewood Cliffs, NJ).
10. Tabor, C. W. & Tabor, H. (1984) *Annu. Rev. Biochem.* **53,** 749–790.
11. Geiger, L. E. & Morris, D. R. (1978) *Nature (London)* **272,** 730–732.
12. Ames, B. N. & Dubin, D. T. (1960) *J. Biol. Chem.* **235,** 769–775.
13. Feuerstein, B. G., Williams, L. D., Basu, H. S. & Marton, L. (1991) *J. Cell. Biochem.* **46,** 37–47.
14. Pochon, F. & Cohen, S. S. (1972) *Biochem. Biophys. Res. Commun.* **47,** 720–726.
15. Khan, A. U., Gebauer, P. & Hager, L. P. (1983) *Proc. Natl. Acad. Sci. USA* **80,** 5195–5197.
16. Kanofsky, J. R. (1984) *J. Biol. Chem.* **259,** 5596–5600.
17. Corey, E. J., Mehrotra, M. M. & Khan, A. U. (1987) *Biochem. Biophys. Res. Commun.* **145,** 842–846.
18. Corey, E. J., Mehrotra, M. M. & Khan, A. U. (1987) *Science* **236,** 68–69.
19. Khan, A. U. (1991) *Int. J. Quantum Chem.* **39,** 251–267.
20. Lee, P. C. C. & Rodgers, M. A. (1987) *J. Photochem. Photobiol.* **45,** 79–86.
21. Piette, J. (1991) *J. Photochem. Photobiol. B:Biol.* **11,** 241–260.
22. Di Mascio, P., Wefers, H., Do-Thi, H.-P., Lafleur, H. & Sies, H. (1989) *Biochim. Biophys. Acta* **1007,** 151–157.
23. Blazek, E. R., Peak, J. G. & Peak, M. J. (1989) *Photochem. Photobiol.* **49,** 607–613.
24. Tabor, H., Tabor, C. W. & Irreverre, F. (1973) *Anal. Biochem.* **55,** 457–467.
25. Frimer, A. A., ed. (1985) *Singlet O_2* (CRC, Boca Raton, FL), Vol. 1–4.
26. Imlay, J. A. & Linn, S. (1988) *Science* **240,** 1302–1309.
27. Minton, K. W., Tabor, H. & Tabor, C. W. (1990) *Proc. Natl. Acad. Sci. USA* **87,** 2851–2855.
28. Khan, A. U., Di Mascio, P., Medeiros, M. H. G. & Wilson, T. (1992) *Proc. Natl. Acad. Sci. USA* **89,** 11428–11430.

Proc. Natl. Acad. Sci. USA
Vol. 89, pp. 11428–11430, December 1992
Biophysics

Spermine and spermidine protection of plasmid DNA against single-strand breaks induced by singlet oxygen

(polyamines)

AHSAN U. KHAN†, PAOLO DI MASCIO‡, MARISA H. G. MEDEIROS‡, AND THÉRÈSE WILSON§

†Department of Pathology, Harvard Medical School, Boston, MA 02115; ‡Instituto de Quimica, Universidade de Sao Paulo, CP 20780, 01498 Sao Paulo, Brazil; and §Department of Cellular and Developmental Biology, Harvard University, Cambridge, MA 02138

Communicated by Michael Kasha, August 31, 1992 (received for review June 23, 1992)

ABSTRACT **Oxidative damage to DNA induced by singlet molecular oxygen ($^1O_2^*$) includes single-strand breaks, which the biologically occurring $^1O_2^*$ quenchers spermine and spermidine are shown to prevent. These polyamines at a physiological concentration (10 mM) reduce the percentage of the open circular form of pBR322 plasmid DNA, which is generated at the expense of the native supercoiled form when the plasmids are incubated with a chemical source of $^1O_2^*$, the water-soluble endoperoxide of 3,3′-(1,4-naphthylidene)dipropionate. Spermine and spermidine can be expected to protect DNA against other damaging effects of $^1O_2^*$.**

Harmful biological effects of molecular oxygen in its $^1\Delta_g$ singlet excited state ($^1O_2^*$) have long been known. These include damage to the genetic material, which results in mutations and loss of transforming activity. $^1O_2^*$ reacts selectively with deoxyguanosine; oxidized guanine residues lose base-pairing specificity (see ref. 1 for a recent review and discussion).

Resolving an earlier controversy, Di Mascio *et al.* (2) and Blazek *et al.* (3) demonstrated independently and unambiguously in 1989 that $^1O_2^*$ also induces single-strand breaks in DNA. Among other findings, these authors showed that exposure to $^1O_2^*$ generates the open circular (OC) form of plasmid pBR322 at the expense of the supercoiled (SC) form of this plasmid. In these experiments, $^1O_2^*$ was produced in three different ways: by photosensitization with an external sensitizer (2, 3); by a microwave discharge through an oxygen stream (2); or chemically, by the decomposition of a water-soluble endoperoxide (2). That $^1O_2^*$ has a role in breaking the DNA backbone was supported by two observations: (*i*) replacing H_2O by ^2H_2O in the buffer increases the percentage of OC generated (2, 3), in keeping with the longer lifetime of $^1O_2^*$ in ^2H_2O (4); and (*ii*) the presence of sodium azide, a very efficient quencher of $^1O_2^*$, protects the native supercoiled form (3). These results have since been confirmed and extended (5–7).

It therefore seemed that the appearance of single-strand breaks in pBR322 DNA, induced by chemically generated $^1O_2^*$, would provide a sensitive and convenient way of testing the hypothesis presented in the companion paper (8)—namely, that polyamines serve to protect DNA *in vivo* against damage by $^1O_2^*$.

MATERIALS AND METHODS

Generation of Singlet Oxygen. Singlet oxygen ($^1O_2^*$) was generated by the thermal dissociation of the water-soluble endoperoxide ($NDPO_2$) of 3,3′-(1,4-naphthylidene)dipropionate (NDP), as described (9). This process generates singlet molecular oxygen ($^1\Delta_g$) in a high yield.

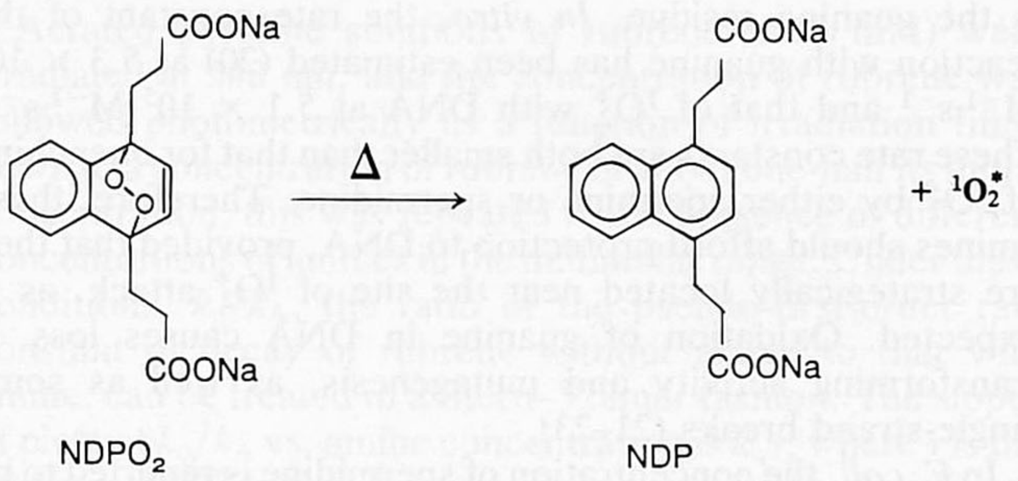

Plasmid Preparation. The HB101 strain of *Escherichia coli* was transformed by plasmid pBR322 using a calcium chloride procedure, essentially as reported (2). Cells were spread on ampicillin (100 μg/ml) agar plates and incubated overnight at 37°C. Transformed *E. coli* cells were grown in LB medium to a cell density of ≈10^9 cells per ml. Plasmid DNA was purified using the Qiagen plasmid kit, pack 500 (Qiagen, Studio City, CA). The plasmid preparation contained ≈85% form I (SC), ≈10% form II (OC), and ≈5% DNA fragments.

Exposure of DNA to $^1O_2^*$, With or Without Inhibitors. Two micrograms (20 μl) of pBR322 DNA was exposed to 10 mM (10 μl) $NDPO_2$ in deaerated 50 mM sodium phosphate buffer in H_2O at pH 7.4 (total volume 200 μl). To study inhibitor effects, some of the solutions contained 10 mM freshly dissolved spermine or spermidine (as polyhydrochlorides), 10 mM histidine, or 1 mM sodium azide (20 μl each), in addition to 10 mM $NDPO_2$. The following three controls were also performed: plasmid alone, plasmid plus 50 mM NDP (the parent compound of $NDPO_2$ and a product of its decomposition), or plasmid plus 10 mM spermine and 10 mM spermidine. In all cases, incubation was at 37°C for 100 min with shaking.

Plasmid Treatment After $^1O_2^*$ Exposure. Separation of the different conformations of pBR322 DNA, form I (SC, native conformation), form II (OC, resulting from single-strand break), and form III (linear DNA, resulting from double-strand breaks), was performed by gel electrophoresis, using 0.7% agarose gels in a horizontal gel electrophoresis chamber at 30 mA for 120 min in 89 mM Tris borate/2 mM EDTA buffer. DNA (10 μl, 100 ng) was mixed with 2 μg of gel loading buffer (15% Ficoll type 400/0.25% bromophenol blue) and applied to the gel. After gel electrophoresis, the DNA bands were stained with ethidium bromide and visualized by fluorescence in a UV (Fotodyne 440) DNA transilluminator system. In the experiments presented in Fig. 2, the negative of a Polaroid (type 55P/N) photograph of the gel was scanned with an E-C Apparatus Corporation (St. Petersburg, FL) densitometer.

The publication costs of this article were defrayed in part by page charge payment. This article must therefore be hereby marked "*advertisement*" in accordance with 18 U.S.C. §1734 solely to indicate this fact.

Abbreviations: OC, open circular; SC, supercoiled; NDP, 3,3′-(1,4-naphthylidene)dipropionate; $NDPO_2$, endoperoxide of NDP.

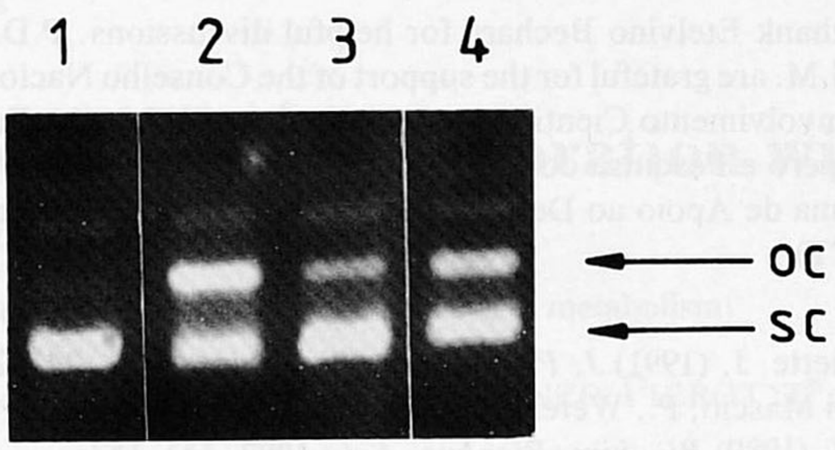

FIG. 1. Electrophoretic separation of pBR322. Singlet oxygen-induced damage and protective effect of spermine, spermidine, and sodium azide. Lane 1, pBR322 plus NDP (50 mM), spermine (5 mM), and spermidine (5 mM); lane 2, pBR322 plus $NDPO_2$ (10 mM); lane 3, pBR322 (10 mM) plus NaN_3 (1 mM); lane 4, pBR322 plus $NDPO_2$ (10 mM), spermine (5 mM), and spermidine (5 mM).

RESULTS AND DISCUSSION

Inspection of Figs. 1 and 2 confirms, first of all, that singlet oxygen induces single-strand breaks in DNA. The percentage of single-strand breaks, resulting in the OC form of plasmid pBR322, rose from 9.7% ± 2.6% in the pBR322 controls to 35% upon incubation with $NDPO_2$ (Fig. 2), confirming previous work (2). Both sets of results, obtained with different preparations of plasmids, also show that neither NDP, the product of the endoperoxide decomposition, spermidine, nor spermine increases the percentage of the OC form of DNA. On the other hand, both sets of results show that 1 mM sodium azide protects the SC form of the plasmid against damage by $^1O_2^*$, confirming the effect of this well-known $^1O_2^*$ quencher. Also as expected, replacing H_2O by ^2H_2O in the

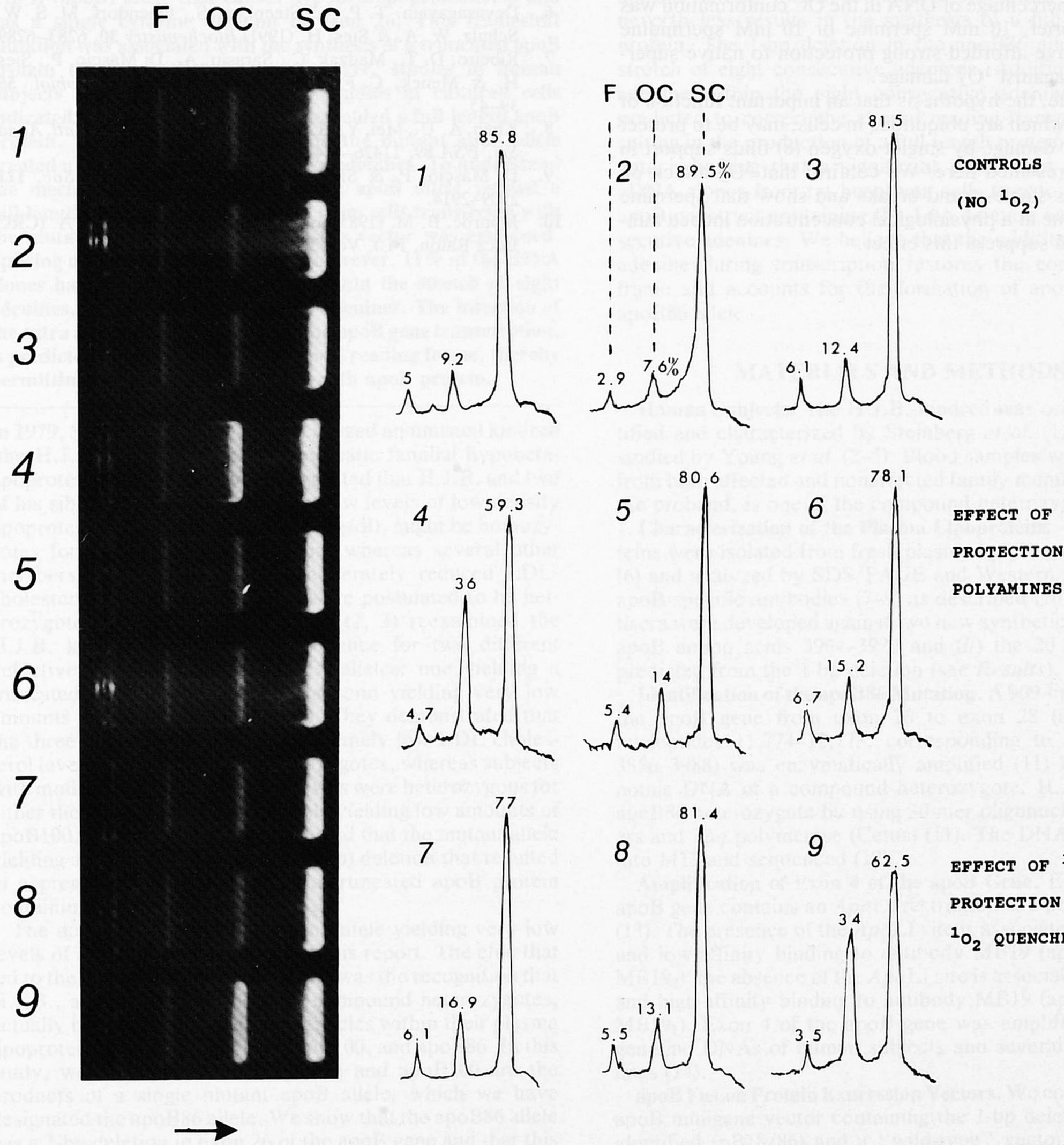

FIG. 2. Gel electrophoresis of plasmid pBR322 after exposure to $^1O_2^*$ generated by the thermal decomposition of the endoperoxide $NDPO_2$, as described in *Materials and Methods*. Effect of the polyamines spermine and spermidine and of the known $^1O_2^*$ quenchers histidine and sodium azide. The DNA is present in two conformations, SC and OC, and as fragments (F). The percentage of DNA in the different forms is indicated next to each peak. Lane 1, pBR322 control; lane 2, pBR322 plus 50 mM NDP; lane 3, pBR322 plus 10 mM spermine and 10 mM spermidine; lane 4, pBR322 plus 10 mM $NDPO_2$; lane 5, pBR322 plus 10 mM $NDPO_2$ and 10 mM spermine; lane 6, pBR322 plus 10 mM $NDPO_2$ and 10 mM spermidine; lane 7, pBR322 plus 10 mM $NDPO_2$ and 10 mM histidine; lane 8, pBR322 plus 10 mM $NDPO_2$ and 1 mM NaN_3; lane 9, pBR322 plus 10 mM $NDPO_2$.